RSC Advances

PAPER

View Article Online
View Journal | View Issue

Open Access Article. Published on 20 November 2024. Downloaded on 10/21/2025 6:07:38 AM.
This article is licensed under a Creative Commons Attribution-NonCommercial 3.0 Unported Licence.

Check for updates

Cite this: *RSC Adv.*, 2024, **14**, 36980

Research on TNTON/DNTF eutectic characteristics: an exploration of low eutectic mixture based melt-cast explosive carriers†

Xinyu Feng,[a] Qi Xue,[a] Junlin Zhang,[ab] Kaidi Yang,[a] Kunkai Wang,[a] Bozhou Wang *[ab] and Fuqiang Bi*[ab]

To modify the sensitivity and melting point of the casting of DNTF, a eutectic system of insensitive explosive 3,5,5-trinitro-1,3-oxazinane (TNTON) and DNTF was prepared through a new method. The melting and liquefaction processes of TNTON/DNTF at different ratios were investigated, and a *T*–*x* phase diagram was established. The melting and decomposition processes of TNTON, DNTF, and TNTON/DNTF eutectic at different heating rates were compared, while the sensitivity tests were conducted to study the desensitizing effect of TNTON on DNTF. Using EXPLO-5 software, the detonation performance of the TNTON/DNTF eutectic was calculated. The experimental results show that the stoichiometric composition of the TNTON/DNTF eutectic is 58.26 : 41.74, with an average melting point of 69 °C. With the increase of heating rate, both the melting and decomposition reactions are delayed. According to the activation energy (E_a) curve, the thermal decomposition is through an autocatalytic process. The impact and friction sensitivity of the TNTON/DNTF eutectic are 38 J and 252 N, respectively. Theoretical density of the TNTON/DNTF eutectic is 1.906 g cm^{-3}, and the calculated detonation velocity is 8921 m s^{-1}. The TNTON/DNTF eutectic exhibits good thermal stability and can significantly reduce the sensitivity of DNTF while maintaining its high energy level. The detonation performance of TNTON/DNTF low eutectic cast explosive is better than that of TNT based cast explosive.

Received 27th May 2024
Accepted 19th October 2024

DOI: 10.1039/d4ra03904a

rsc.li/rsc-advances

1 Introduction

Melt-cast explosives are currently one of the main charging methods for warheads,[1–3] but the existing formula of melt-cast explosives based on a single explosive molecule (such as TNT[4]) has obvious shortcomings in terms of energy, safety, charging quality, and mechanical properties[5–7] as a carrier. The melt-cast process normally includes the addition of solid high-energy components into liquid molten carrier explosives and could effectively improve the final detonation and molding performances. Despite the low energy, poor mechanical properties, poor safety, and high toxicity, TNT remains the most important and widely used carrier for molten explosives to date. During the last few decades, continuous efforts in the exploration of new casting carriers to replace TNT were made,[8] among which, DNTF[9] has attracted widespread attention worldwide.

Energetic materials based on tandem furazan–furoxan framework often exhibit superior energetic performance due to their high enthalpy of formation,[10,11] and DNTF is the most representative and efficient material with the advantages of prominent energetic properties (density of 1.937 g cm^{-3}, detonation velocity of 9250 m s^{-1}, detonation pressure of 41.1 GPa, heat decomposition temperature of 253.6 °C under atmospheric pressure, and 5 s explosion point of 308 °C), outstanding enthalpy of formation, as well as high nitrogen content.[9] With a melting point of 110 °C, DNTF has been regarded as one of the most important casting carriers for future melt-cast explosives. However, in current stage, the high sensitivity characteristics of DNTF still seriously hinder its large-scale application in casting explosives and propellants. Therefore, some research groups, including us, have proposed that the exploration of low eutectic mixture based on DNTF and other energetic components could be a promising solution to this problem.[12]

Energetic eutectics refer to energetic mixtures formed by mixing two or more energetic compounds, where one or more components are in a molten state, and other components dissolve in it, the energetic eutectics formed has a melting point lower than each of its single component.[13] Energetic eutectics formed through the addition of a second component will compensate for the shortcomings of single-component explosives in terms of melting point and sensitivity, which has become a hot topic of research in recent years.[14–16] In 2020 and 2022, we reported the preparation of two eutectic systems by mixing BOM[3] and (3,5-dinitro-1,3-oxazinan-5-yl) methyl nitrate

[a]Xi'an Modern Chemistry Research Institute, Xi'an, 710065, China. E-mail: bifuqiang@msn.com; wbz600@163.com

[b]State Key Laboratory of Fluorine & Nitrogen Chemicals, Xi'an, 710065, China

† Electronic supplementary information (ESI) available. See DOI: https://doi.org/10.1039/d4ra03904a

© 2024 The Author(s). Published by the Royal Society of Chemistry

Open Access Article. Published on 20 November 2024. Downloaded on 10/21/2025 6:07:38 AM.
This article is licensed under a Creative Commons Attribution-NonCommercial 3.0 Unported Licence.

(TNOP)[17] with DNTF and achieved a eutectic temperature of 75.5 °C and 95.4 °C respectively. But the sensitivities and energetic performances of the eutectic mixtures have not yet met our expectations.

TNTON[18] is an excellent nitrogen-containing cyclic energetic compound with a density of 1.78 g cm^{-3}, a melting point of 89 °C, and a heat decomposition temperature of 231 °C, exhibiting good stability[19] and low sensitivity (38 J, 360 N). Compared to most widely applied explosives as casting carriers, TNTON demonstrates a better overall performance, which ensures a more ideal energy level for the TNTON/DNTF eutectic. This article utilizes the high melting point and low sensitivity characteristics of TNTON to prepare a binary mixture system with DNTF, trying to reduce the final casting process temperature and sensitivity, meanwhile maintain a high energetic level to meet the requirements for advanced warheads and propellants. It is noteworthy that a new way to prepare the binary mixture has been reported in this article, which is different from the traditional strategies. By avoiding heating/melting operations and abandoning the direct grinding of solid powders, this new method significantly improved the safeties. This research aims to establish the *T*–*x* phase diagram of the TNTON/DNTF binary system, determine the composition and melting temperature of the eutectic, and analyze the influence of different heating rates on the melting and decomposition processes of the eutectic through DSC,[20] as well as carry out the sensitivity tests and detonation performance calculations of the eutectic, in order to achieve the purpose of reducing the sensitivity of DNTF, adjusting the melting point of DNTF, and maintaining its high energy level (Fig. 1).

2 Experimental section

2.1 Reagents and instruments

2.1.1 Reagents. Nitromethane, acetonitrile, petroleum ether, analytical grade, Sinopharm Chemical Reagent Co., Ltd; sodium hydroxide, sodium persulfate, sodium nitrite, concentrated nitric acid, analytical grade, Chengdu Kelon Chemical Co., Ltd; *tert*-butylamine, tetrafluoroacetic anhydride, potassium ferricyanide, analytical grade, Shanghai Aladdin Biochemical Technology Co., Ltd; Polyformaldehyde, analytical grade, Yinfeng Bioengineering Group Co., Ltd; DNTF, purity ≥ 99%, Xi'an Modern Chemistry Research Institute; TNTON, self-made according to literature method,[18] purity ≥99%.

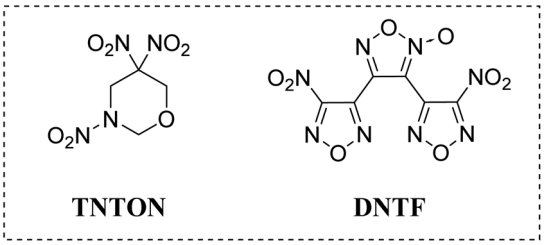

Fig. 1 Chemical structures of the studied compounds TNTON and DNTF.

2.1.2 Instruments. 449C Differential Scanning Calorimeter, NETZSCH Gerätebau GmbH; WL-1 Impact Sensitivity Tester and WM-1 Friction Sensitivity Tester, Xi'an Institute of Modern Chemistry.

2.2 Compatibility test of TNTON/DNTF and preparation of eutectic

Eleven groups of mixtures of TNTON and DNTF with mass ratios of 0 : 10, 1 : 9, 2 : 8, 3 : 7, 4 : 6, 5 : 5, 6 : 4, 7 : 3, 8 : 2, 9 : 1, 10 : 0 were weighed in small beakers, with a total mass of 1 g for each group, named from 1$^{\#}$ to 11$^{\#}$. As shown in Fig. 2, each group of mixtures was completely dissolved in acetone to form a saturated solution, stirred for 5 min, and then allowed to slowly solidify at room temperature as the solvent evaporated. After complete solidification, petroleum ether was added to thoroughly wet the solid, followed by grinding the solid into a powder form dispersed in petroleum ether. After grinding, the mixture was filtered, air-dried at room temperature, and the resulting powders were collected for related tests. Based on the *T*–*x* phase diagram and other analysis results, the composition of the lowest eutectic was determined, and TNTON/DNTF eutectic was prepared using the same method.

2.2.1 Caution. although we did not encounter any unexpected explosions and hazards in the course of this research, small scale and safety equipments such as protective gloves and coats, face shield, and explosion-proof baffle are recommended when handling DNTF and TNTON.

A sample with a mass ratio of 1 : 1 of TNTON and DNTF was subjected to DSC testing. The compatibility was evaluated according to the thermal analysis evaluation compatibility standards proposed by Honeywell Company in the United States,[21,22] using the maximum exothermic peak temperature change Δt_p for evaluation.

$$\Delta t_p = t_{p1} - t_{p2} \tag{1}$$

where t_{p1} is the maximum exothermic peak temperature of the reference system; t_{p2} is the maximum exothermic peak temperature of the mixed system.

The compatibility evaluation standard is shown in Table 1,[23,24] and the DSC curves of TNTON and DNTF and their mass ratio of 1 : 1 mixture are shown in Fig. 3. As shown in Fig. 3, the thermal decomposition peak of TNTON/DNTF mixed system is 2.8 °C

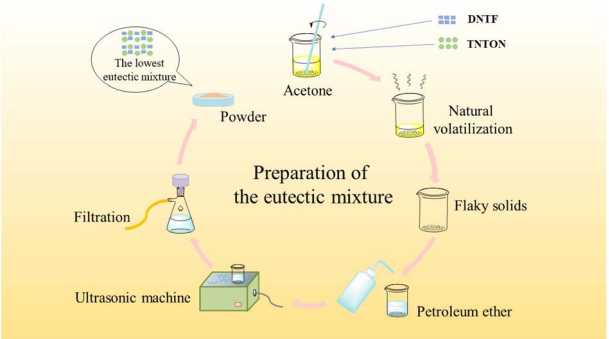

Fig. 2 Preparation of the eutectic mixture.

Open Access Article. Published on 20 November 2024. Downloaded on 10/21/2025 6:07:38 AM.
This article is licensed under a Creative Commons Attribution-NonCommercial 3.0 Unported Licence.

Table 1 Standard for evaluating compatibility with Δt_p

Δt_p/°C	Rating	Note
0–3	A	Mixed system compatibility
3–5	B	The hybrid system is slightly sensitive and can be used for a short time
6–15	C	The hybrid system is sensitive. It's best not to use it
>15	D	Mixed system dangerous, strictly prohibited use

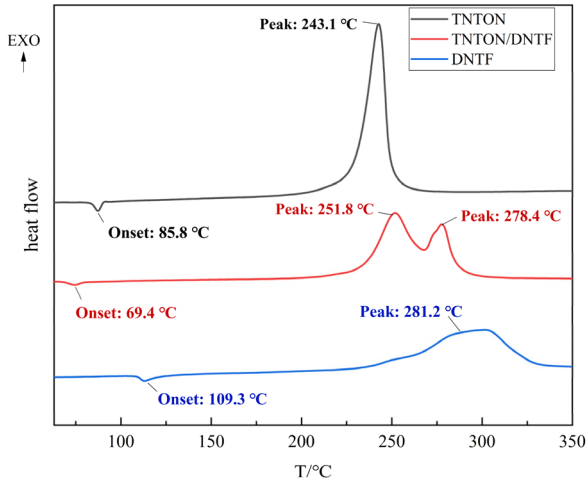

Fig. 3 DSC curves of TNTON and DNTF.

earlier than that of DNTF. According to the compatibility evaluation criteria in Table 1, TNTON and DNTF are compatible.

2.3 Performance testing

2.3.1 DSC analysis. (1) DSC analysis was performed on samples of TNTON/DNTF mixtures with different ratios, with a heating rate of 10 K min^{-1}, a temperature range of 25–400 °C, a sample size of 0.4–1 mg, under nitrogen atmosphere (30 mL min^{-1}), using a sealed gold crucible; (2) the prepared TNTON/DNTF eutectic was subjected to DSC analysis testing at different heating rates (5, 10, 15, 20 K min^{-1}), with a temperature range of 25–400 °C, a sample size of 2–4 mg, under nitrogen atmosphere (30 mL min^{-1}), using a sealed gold crucible.

2.3.2 Sensitivity analysis. According to the method 601.1 of GJB772A-97, the impact sensitivity and friction sensitivity of TNTON, DNTF, and TNTON/DNTF eutectic were tested using a WL-1 type impact sensitivity tester and a WM-1 type friction sensitivity tester: the impact sensitivity test used a 5 kg falling weight, a drop height of 25 cm, and a charge of 500 mg; the friction sensitivity test used a pressure of 3.92 MPa, a pendulum angle of 90°, and a charge of 500 mg.

3 Results and discussion

3.1 Binary phase diagram of TNTON/DNTF system

DSC tests were conducted on TNTON/DNTF mixtures with mass ratios of 0 : 10, 1 : 9, 2 : 8, 3 : 7, 4 : 6, 5 : 5, 6 : 4, 7 : 3, 8 : 2, 9 : 1, 10 : 0, represented by 1#, 2#, 3#, 4#, 5#, 6#, 7#, 8#, 9#, 10#, and 11# (Fig. 4).

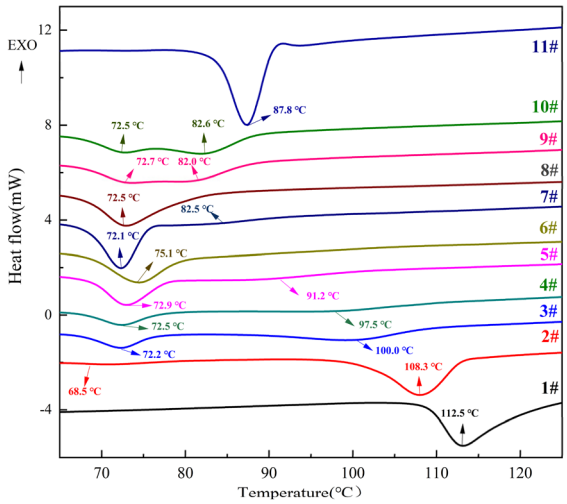

Fig. 4 DSC spectra of TNTON/DNTF with different mass ratios.

Pure TNTON and DNTF each produced a single endothermic peak, indicating that the melting points of TNTON and DNTF are 89 °C and 110 °C, respectively. The DSC curves of the TNTON/DNTF mixtures showed two endothermic peaks, the first of which is the melting peak of the eutectic, and the second is the liquefaction peak of the remaining components. As the content of TNTON increased, the liquefaction temperature of the binary system first decreased and then increased. As shown in Fig. 4, the low eutectic temperature of different systems remained approximately constant, ranging from 67.9 to 70.6 °C, with an average low eutectic temperature of 69.0 °C. This is due to the lowering of the freezing point phenomenon caused by the chemical potential of any component in the mixed solution system being lower than that of the pure substance under the same temperature and pressure conditions, according to the colligative properties of dilute solutions.[24] The absorption peaks gradually merged into a single absorption peak at a component mass ratio of 5 : 5, indicating that this mixture system is very close to the composition of the TNTON/DNTF eutectic.

According to the definition of DSC determination of melting point, the phase change temperature (melting point) of pure substance (or low eutectic) melting should be the initial temperature t_0 of the tangent extrapolation of the front edge of the melting heat absorption peak, and the temperature difference between the temperature of complete melting (or liquefaction) T_e and T_0 is the so-called "melting range", the melting range on the DSC curve is related to the rate of heating. To obtain the accurate liquefaction temperature of the mixed system, it is necessary to correct the obtained DSC temperatures (Fig. 5).

The temperature gap between the end temperature T_e and the starting temperature T_0 of the melting peak of the eutectic mixture was taken as the correction amount to determine the complete liquefaction temperature T_L of the mixture in Fig. 5. The correction formula for the liquefaction temperature is shown in eqn (2).

 © 2024 The Author(s). Published by the Royal Society of Chemistry

Open Access Article. Published on 20 November 2024. Downloaded on 10/21/2025 6:07:38 AM.
This article is licensed under a Creative Commons Attribution-NonCommercial 3.0 Unported Licence.

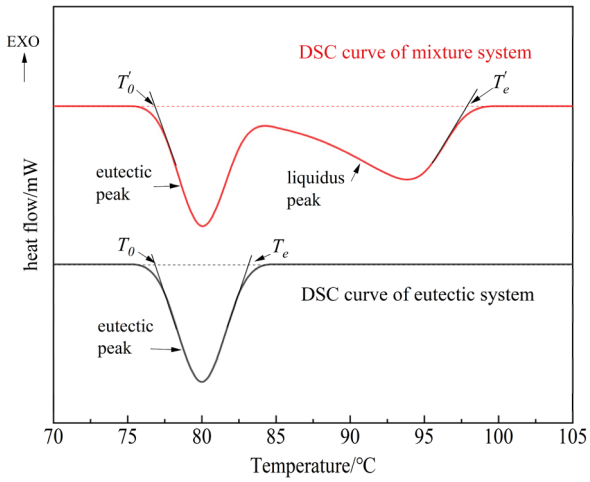

Fig. 5 Schematic diagram of liquefaction temperature obtained from DSC curves of the binary system.[16,24,25]

$$T_L = T_e' - (T_e - T_0) \quad (2)$$

where T_L is the complete liquefaction temperature of the mixture; T_e' is the end temperature of the liquefaction peak of the mixed system DSC curve; T_0 is the starting temperature of the eutectic peak; T_e is the end temperature of the eutectic peak.

The liquefaction temperature and component content of the binary system have the following relationship:[24]

$$\ln \text{ ч}_1 = \frac{\Delta H_{12}}{R}\left(\frac{1}{T_1^0} - \frac{1}{T_1}\right) \quad (3)$$

$$\ln \text{ ч}_2 = \frac{\Delta H_{21}}{R}\left(\frac{1}{T_2^0} - \frac{1}{T_2}\right) \quad (4)$$

where x_1 and x_2 are the molar fractions of components 1 and 2 in the mixed system, respectively; T_1^0 and T_2^0 are the melting points of components 1 and 2 in the mixed system (K); T_1 and T_2 are the liquefaction temperatures of components 1 and 2 in the mixed system(K); ΔH_{12} is the enthalpy of melting of component 1 in the presence of component 2(J mol^{-1}); ΔH_{21} is the enthalpy of melting of component 2 in the presence of component 1 (J mol^{-1}); R is the gas constant.

According to eqn (2), the liquefaction temperature of the mixed components is obtained, and combined with equation eqn (3) or eqn (4), a plot of the liquefaction temperature T_L *versus* component content x_i (the T–x phase diagram of the binary eutectic)is made.[26]

The DSC curve characteristic data of different molar ratio TNTON/DNTF mixtures are shown in Table 2. T_{eu} is the starting temperature of the low eutectic peak, that is, the low eutectic temperature; T_e' is the end temperature of the liquefaction peak on the DSC curve of the mixed system; T_L is the corrected temperature of the mixture after complete liquefaction. According to Fig. 4, the 6# group with a molar ratio of n_{TNTON} : n_{DNTF} = 58.43 : 41.57 has only one melting peak in its DSC curve, indicating that the mixture system forms a complete eutectic at this ratio. Therefore, when calculating the liquefaction temperature of the mixed system, the melting range of 14 °C of this mixture system peak is used for calculation.

Table 2 DSC characteristic values of the TNTON/DNTF mixed system with different molar ratios

Samples	TNTON/DNTF Mass ratio	TNTON/DNTF Molar ratio	T_{eu}/°C	T_L/°C	T_e'/°C
1	0 : 1	0 : 100.00	109.3	109.3	—
2	1 : 9	13.51 : 86.49	68.4	104.3	118.3
3	2 : 8	26.00 : 74.00	68.8	97.3	111.3
4	3 : 7	37.59 : 62.41	68.4	86.6	100.6
5	4 : 6	48.37 : 51.63	70.6	77.8	91.8
6	5 : 5	58.43 : 41.57	69.4	69.4	83.4
7	6 : 4	67.83 : 32.17	70.1	73.6	87.6
8	7 : 3	76.63 : 23.37	68.7	77.5	91.5
9	8 : 2	84.90 : 15.10	67.9	80.9	94.9
10	9 : 1	92.67 : 7.33	68.4	84	98
11	1 : 0	100.00 : 0	85.8	85.8	—

According to the data in Table 2, a plot of the liquification temperature t_L *versus* component content x gives the T–x phase diagram of the binary eutectic. Fig. 6 shows the phase diagram of TNTON content *versus* temperature for the TNTON/DNTF binary mixture. The points in the diagram are the measured values, and the solid line is the fitted curve. It can be observed that the two fitted liquification temperature curves intersect with the fitted melting temperature curve at one point, with the coordinates x(TNTON) = 0.584, indicating that the composition of the TNTON/DNTF eutectic is $x_{TNTON} : x_{DNTF}$ = 58.4 : 41.6.

By performing linear regression of ln x, $1/T$ where x is the molar fraction of TNTON or DNTF in the mixed system, and T is the liquification temperature of TNTON or DNTF in the mixed system, the relationships for DNTF and TNTON regression are obtained as shown in eqn (5) and (6):

$$\ln x_{DNTF} = 7.1586 - 2750/T,\ R = 0.997 \quad (5)$$

$$\ln x_{TNTON} = 10.953 - 3934.9/T,\ R = 0.998 \quad (6)$$

The low eutectic point of TNTON/DNTF is the intersection point of eqn (5) and (6). Therefore, the molar ratio of TNTON to

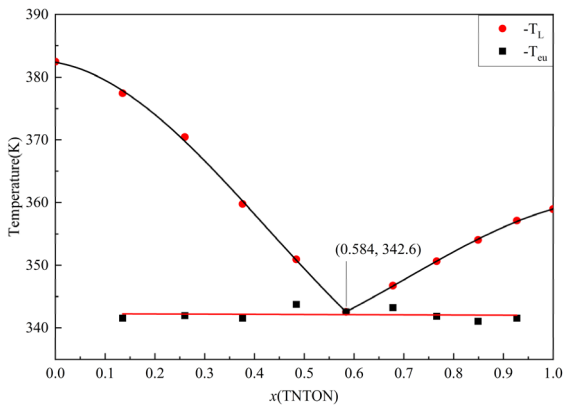

Fig. 6 The phase diagram of the TNTON/DNTF binary composition.

Open Access Article. Published on 20 November 2024. Downloaded on 10/21/2025 6:07:38 AM.
This article is licensed under a Creative Commons Attribution-NonCommercial 3.0 Unported Licence.

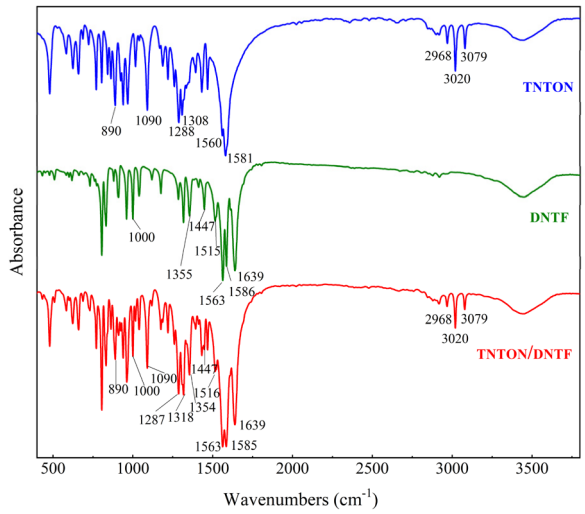

Fig. 7 IR spectra of TNTON, DNTF and the TNTON/DNTF eutectic.

DNTF in the low eutectic of TNTON/DNTF system is 58.26 : 41.74, and the low eutectic temperature is 342.37 K (69.2 ° C).The average T_{eu} of the mixed system in Table 2 is 69 °C (342.15 K) as the low eutectic temperature of the TNTON/DNTF system, and the component content of DNTF or TNTON in the low eutectic can be calculated by taking the T of eqn (5) or (6) as 342.15 K. The content of TNTON in the low eutectic could be obtained by $1 - x_{DNTF}$ while the content of DNTF in eutectic be determined by $1 - x_{TNTON}$.The molar ratio of TNTON to DNTF in the eutectic of TNTON/DNTF system is calculated to be 58.5 : 41.5 and 57.8 : 42.2 according to these two methods respectively. It can be seen from the above results that the composition and temperature of the low eutectic calculated by the three methods are very close, which indicates that the regression calculation method is reliable to calculate the composition and temperature of the low eutectic.

The eutectic composition calculated by the intersection of eqn (5) and (6) is close to the average of the individual component ratios calculated by eqn (5) or (6) alone. Therefore, the molar ratio of TNTON to DNTF in the TNTON/DNTF eutectic is determined to be 58.26 : 41.74, the mass ratio is 49.8 : 50.2, and the eutectic temperature is 69 °C.

Infrared (IR) spectral analysis of the TNTON/DNTF eutectic, as shown in Fig. 7 and Table 3, reveals all major vibrational bands of pure TNTON and DNTF in the eutectic. The peaks of 2968 cm^{-1}, 3020 cm^{-1} and 3079 cm^{-1} are the stretching vibrations of C–H bonds in TNTON, in which the C–O–C fragment in the TNTON ring skeleton has a stretching vibration peak at 1090 cm^{-1}. The peak of vibration at 1000 cm^{-1} corresponds to the stretching vibrations of O–N in the furoxan ring. The bands 1639 cm^{-1}, 1515 cm^{-1} and 1447 cm^{-1} are the skeleton characteristic peaks of furaxan ring, and 1585 cm^{-1}, 1563 cm^{-1}, 1447 cm^{-1}, 1409 cm^{-1} are the skeleton characteristic peaks of furaxan ring. Similarly, NO_2 symmetric and asymmetric stretching vibrations were observed at 1320 ± 40 cm^{-1} and 1550 ± 50 cm^{-1}. According to these results, the functional groups in the eutectic complex were determined to be the same as those in the raw materials, indicating that during the preparation of the TNTON/DNTF mixture, no new chemical bond was formed between the original TNTON and the original DNTF, indicating good material compatibility. In addition, the peak 1308 cm^{-1} is related to TNTON's C–NO_2 symmetric stretching vibration, and this peak moves to 1318 cm^{-1} in the eutectic, which is likely due to the interaction between the two molecules.

Based on Fig. 8, it can be observed that the melting point of TNTON and DNTF is significantly reduced after forming the eutectic mixture, and the onset temperature of thermal decomposition is delayed by nearly 10 °C compared to pure TNTON. This may be due to the intermolecular forces between the two molecules, which make the overall structure more stable, leading to an increased decomposition temperature. Moreover, the decomposition temperature of the DNTF component within the eutectic mixture occurs earlier than that of pure DNTF, which might be due to some decomposition products of TNTON exerting a catalytic effect on the thermal decomposition process of DNTF.

3.2 The effect of heating rate on the melting and decomposition process of TNTON/DNTF eutectic

In order to study the effect of heating rate on the melting of low eutectic, different heating rates of 5, 10, 15, 20 K °C min^{-1} were used to carry out experiments, and the composition ratio of low eutectic was prepared according to the calculation results of T–x phase diagram ($n_{TNTON} : n_{DNTF} = 58.26 : 41.74$). Fig. 9 shows the melting change curve of TNTON/DNTF eutectic at different heating rates, and Fig. 10 shows the DSC curve of the

Table 3 IR spectra of raw TNTON, raw DNTF and the TNTON/DNTF eutectic

	TOTON	DNTF	TNTON/DNTF
C–H stretching	3079, 3020, 2968		3079, 3020, 2968
NO_2(N–NO_2) asymmetric stretching vibration	1581		1585
NO_2(C–NO_2) asymmetric stretching vibration	1560	1515	1563, 1516
NO_2(C–NO_2) symmetric stretching vibration	1308	1355	1318, 1354
NO_2(N–NO_2) symmetric stretching vibration	1288		1287
C–O–C asymmetric stretching vibration	1090		1090
C–NO_2 structural bond C–N stretching	890		890
N–O stretching		1000	1000
Skeletal stretching (furoxan ring)		1639, 1515, 1447	1639, 1516, 1447
Skeletal stretching (furaxan ring)		1585, 1563, 1447, 1409	1585, 1563, 1447, 1409

 © 2024 The Author(s). Published by the Royal Society of Chemistry

Open Access Article. Published on 20 November 2024. Downloaded on 10/21/2025 6:07:38 AM.
This article is licensed under a Creative Commons Attribution-NonCommercial 3.0 Unported Licence.

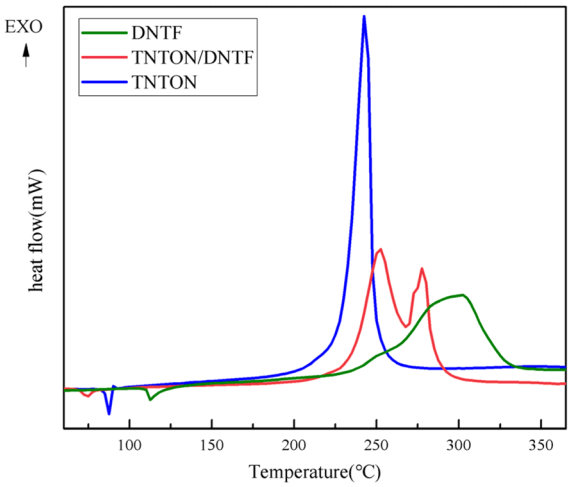

Fig. 8 DSC curves of TNTON, DNTF and TNTON/DNTF eutectic.

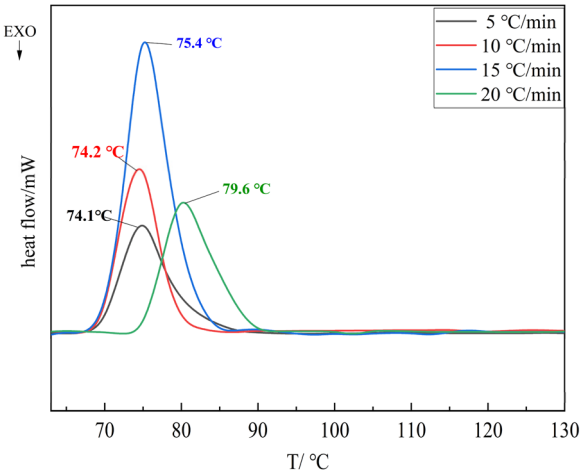

Fig. 9 DSC curves of melting process of TNTON/DNTF eutectic at different heating rates.

decomposition process. As can be seen from Fig. 9 and 10, with the increase of heating rate, both the start time and peak value of melting reaction and decomposition reaction are delayed. The peak melting temperature of low eutectic is delayed from 74.1 °C at 5 °C min^{-1} to 79.6 °C at 20 °C min^{-1}, and the average peak melting temperature is 75.8 °C. The delay in peak temperature of low eutectic point is mainly caused by the overheating phenomenon of low eutectic melting caused by high heating rate. Under constant pressure conditions, the temperature of solid–liquid equilibrium is called the equilibrium melting point, and when the solid phase reaches the equilibrium melting point, the phenomenon of non-melting is called overheating. When the melting process of the eutectic is studied by DSC, the heating furnace and the sample are close to the heat equilibrium state at the low heating rate, but the increase of the heating rate will cause the internal temperature release of the sample to be uneven and overheating. The faster the heating rate, the more obvious the overheating phenomenon.

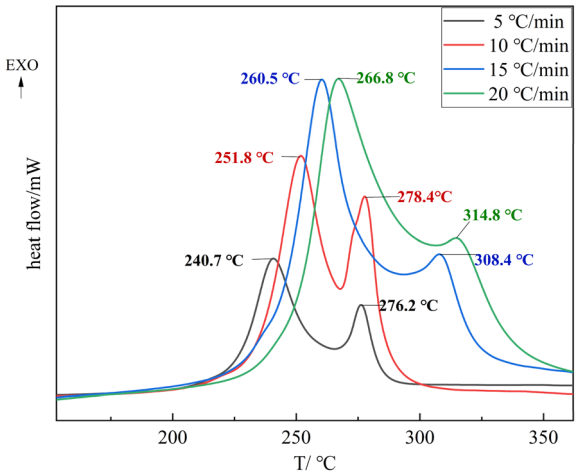

Fig. 10 DSC curve of decomposition process of TNTON/DNTF eutectic at different heating rates.

From Fig. 9, it can be seen that the two stages of the decomposition process of TNTON/DNTF eutectic are delayed at different heating rates. The first stage of the decomposition peak temperature ranges from 240.7 to 266.8 °C, with an average decomposition peak temperature of 255.0 °C, indicating good thermal stability. The difference between the thermal decomposition peak temperature and the average melting peak temperature is 179.2 °C, which is significant, indicating that TNTON/DNTF eutectic has good process applicability as a casting explosive carrier.[8]

Resulting DSC curves were applicated to calculate the kinetic parameters such as apparent E_a. The software NETZSCH Kinetics NEO was used to explore the optimum simulation method, which obtains many kinds and different methods has a huge impact on the parameter results. DSC curves at different heating rates were employed at four different heating rates of 5, 10, 15 and 20 K min^{-1}. The decomposition temperatures increased with the increase of the heating rates. We tried several thermal decomposition equations such as Kissinger, Ozawa and Friedman. The last method is most suitable for the molecular decomposition model and the correlation factor is $R^2 = 0.984$. As can be seen from the Fig. 11, with the progress of thermal decomposition reaction, the E_a has a trend of decreasing, indicating that the thermal decomposition product catalyzes its further decomposition, which is an "autocatalytic decomposition process". The above-mentioned values have been showed in ESI Table S1† for respectively.

3.3 Performance of TNTON/DNTF eutectic

The impact sensitivity and friction sensitivity test results of TNTON, DNTF, and TNTON/DNTF eutectic are shown in Table 4. In addition, the detonation performance of TNTON/DNTF eutectic was calculated using EXPLO-5 software.[34] The calculation results were compared with the detonation performance parameters of common casting explosive carriers. As can be seen from Table 4, the friction sensitivity of TNTON/DNTF eutectic is 252 N, and the impact sensitivity is 38 J, showing

Open Access Article. Published on 20 November 2024. Downloaded on 10/21/2025 6:07:38 AM.
This article is licensed under a Creative Commons Attribution-NonCommercial 3.0 Unported Licence.

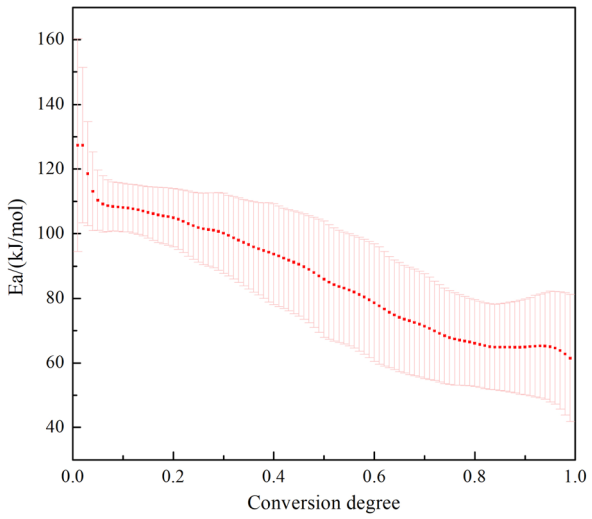

Fig. 11 The relationship of apparent E_a on the degree of conversion TNTON/DNTF eutectic.

a significant improvement in safety performance compared to DNTF. The density of TNTON/DNTF eutectic is 1.906 g cm^{-3}, higher than most of single-component casting explosives; the thermal decomposition starting temperature is 234.6 °C, close to TNT; the detonation velocity is 8921 m s^{-1}, and the detonation pressure is 36.6 GPa. The energy level is higher than that of current common explosive carriers such as DNAN, DNP, 5,5′-ethanitrat-3,3′-bi-1,2,4-oxadiazole (BOM), and the detonation velocity is comparable to that of 1-methyl-2,4,5-trinitroimidazole (MTNI), indicating that compared with single-component DNTF, the density and detonation performance of TNTON/DNTF eutectic have not significantly decreased, in the meantime, the presence of TNTON greatly reduces the sensitivity of DNTF, indicating its broad application prospects.

3.4 Theoretical performance of melt cast explosives based on TNTON/DNTF eutectic

Melt cast explosives have a simple filling process, are suitable for filling irregularly shaped warheads, can adjust various properties through formulation, have strong batch production capabilities, and high automation levels. They still have significant advantages among different types of explosives in the foreseeable future. Melt cast explosives with TNT as the carrier accounted for more than 90% of military mixed explosives in the past, but traditional TNT-based melt cast explosives can no longer meet the requirements of new-era weapon equipment. Improving energy, safety performance, mechanical properties, and reducing harm to personnel and the environment are the long-term development goals of melt cast explosives.[35]

To further verify the application prospects of TNTON/DNTF eutectic in the field of melt cast explosives, we also calculated the detonation velocity, detonation pressure, and density of mixed explosives with TNTON/DNTF eutectic replacing TNT as the melt cast carrier, and CL-20, RDX, HMX as solid high-energy components. Considering the rheology,[36,37] process requirements,[5,38] energy[39] and mechanical performance of melt cast explosives, the proportion of solid high-energy components in the mixed explosive system is generally between 40% and 70%,[35,40] TNTON/DNTF eutectic-based mixed explosives with solid high-energy components CL-20, RDX, HMX at carrier proportions of 30%, 40%, 50%, and 60% were studied. The performance of TNT-based mixed explosives with the same formulation was also compared (Fig. 12). For convenience, "M" represents "TNTON/DNTF eutectic". In Fig. 12, the detonation velocity of TNTON/DNTF eutectic-based melt cast explosives is very high, all higher than 8600 m s^{-1}, with a significant improvement compared to TNT-based melt cast explosives. In addition, with the same solid high-energy components, the increase of TNTON/DNTF eutectic content has a small effect on the detonation velocity, and the performance is relatively stable under different formulations. In practical applications, small adjustments in the mixed explosive formulation can also ensure its excellent detonation performance. This indicates that TNTON/DNTF eutectic-based melt cast explosives have better performance than TNT-based melt cast explosives, and TNTON/DNTF eutectic has the potential to become a new type of melt cast explosive carrier for industrial applications (Fig. 12).

As shown in Table 5, The data outside the brackets are the theoretical properties of M-base fusion-cast explosives, and the data inside the brackets are the theoretical properties of TNT based fusion-cast explosives. TNTON/DNTF eutectic cast explosive has high detonation pressure and density. The detonation pressure of M-base fusible cast explosive is all higher

Table 4 Comparison of detonation properties of TNTON/DNTF eutectic and other melt cast explosive carrier

Substrate	ρ/(g cm^{-3})	ΔH_f^0/(kJ mol^{-1})	T_m/°C	T_{dec}/°C	V_{det}/(m s^{-1})	P_{cj}/GPa	FS/N	IS/J
TNTON[18]	1.78	−249	89	231	8322	31.0	360	38
DNTF[9]	1.937	570.0	110	253.6	9250	41.1	82	5
M_{TNTON} : M_{DNTF} 49.8 : 50.2	1.906	84.7	69	234.6	8921	36.6	252	38
TNT[27,28]	1.64	−59.4	80.8	266.5	6940	19.0	353	15
RDX[28]	1.86	92.6	204	235	9014	33.91	120	7.4
DNAN[29–31]	1.54	−184.0	94.6	351.7	5974	9.5	179	—
DNP[15]	1.87	115.2	85	347	8100	29.4	—	—
MTNI[32]	1.8	64.7	94.7	314.9	8800	35.6	—	—
BOM[33]	1.832	−140.3	84.5	183.4	8180	29.4	282	8.6

 © 2024 The Author(s). Published by the Royal Society of Chemistry

Open Access Article. Published on 20 November 2024. Downloaded on 10/21/2025 6:07:38 AM.
This article is licensed under a Creative Commons Attribution-NonCommercial 3.0 Unported Licence.

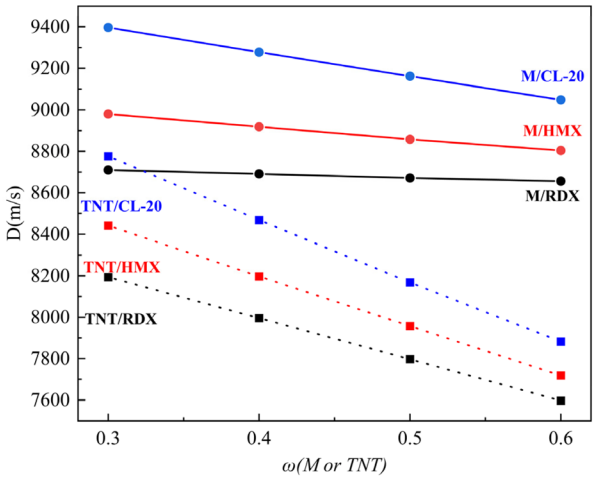

Fig. 12 Detonation velocity of TNTON/DNTF eutectic base (TNT) fused cast explosives.

Table 5 Density, detonation velocity and pressure of TNTON/DNTF eutectic base (TNT) fused cast explosives

	Mass ratio	ρ/(g cm^{-3})	V_{det}/(m s^{-1})	P_{cj}/GPa
M(TNT) : RDX	3 : 7	1.816(1.752)	8710(8194)	33.7(28.6)
	4 : 6	1.822(1.737)	8691(7996)	33.6(27.0)
	5 : 5	1.827(1.722)	8671(7797)	33.3(25.5)
	6 : 4	1.833(1.707)	8656(7597)	33.4(24.1)
M(TNT) : HMX	3 : 7	1.893(1.824)	9198(8441)	36.2(30.8)
	4 : 6	1.888(1.797)	8980(8197)	35.8(28.8)
	5 : 5	1.882(1.771)	8858(7957)	35.2(26.9)
	6 : 4	1.877(1.745)	8804(7718)	34.8(25.1)
M(TNT) : CL-20	3 : 7	1.981(1.905)	9697(8776)	41.0(34.8)
	4 : 6	1.962(1.864)	9397(8468)	39.5(31.9)
	5 : 5	1.943(1.824)	9278(8168)	38.5(29.0)
	6 : 4	1.925(1.787)	9162(7881)	37.3(26.6)

than 33 GPa under different formulations, while that of TNT-based fusible cast explosive is in most cases lower than 30 GPa. The detonation density of M-base fusing cast explosives is above 1.85 g cm^{-3}, while the detonation pressure of TNT base fusing cast explosives is below 1.8 g cm^{-3}. Therefore, the comprehensive properties of TNTON/DNTF-based cast explosives are obviously better than those of TNT based cast explosives.

4 Conclusions

In conclusion, a TNTON/DNTF eutectic was successfully synthesized, which was characterized by a low eutectic temperature of 69 °C and molar ration of 58.26 : 41.74 and mass ratios of 49.8 : 50.2. The average temperature differences between the melting and decomposition peaks under various heating rates is as high as 179.2 °C, which implies the eutectic's favorable processing characteristics for use in casting explosives. The thermal decomposition of TNTON/DNTF eutectic is an autocatalytic process. This eutectic effectively decreased the melting point and sensitivity of DNTF, while preserving its high energy potential. It holds a competitive edge over current explosive carriers, offering enhanced detonation velocity, pressure, and density that surpass those of TNT-based explosives. The similar performance across diverse formulations makes the TNTON/DNTF eutectic as a prospective alternative to TNT in the realm of melt cast explosives.

Data availability

Data supporting the findings of this study are publicly available in the manuscript's references. The data supporting this article have been included as part of the ESI.†

Conflicts of interest

There are no conflicts to declare.

Acknowledgements

This work was supported by the National Natural Science Foundation of China (No. 22205176) and Natural Science Foundation of Shaanxi Province (No. 2024JC-ZDXM-07).

Notes and references

1 B. Zheng, G. Luo, Y. Shu and P. Wang, *Chem. Ind. Eng. Prog.*, 2013, **32**, 1341–1346.
2 N. Liu, S. Zeman, Y.-j. Shu, Z.-k. Wu, B.-z. Wang and S.-w. Yin, *RSC Adv.*, 2016, **6**, 59141–59149.
3 X. Yang, J. Zhou, X. Xing, Y. Huang, Z. Yan, Q. Xue, X. Wang and B. Wang, *RSC Adv.*, 2020, **10**, 26425–26432.
4 Q. H. Wang, *Energetic Mater.*, 2004, **12**, 46–55.
5 Y. Wang, J. H. Rui and S. S. Feng, *J. Beijing Inst. Technol.*, 2011, **31**, 757–760.
6 O. H. Johansen, J. D. Kristiansen and R. Gjersoe, *Propellants, Explos., Pyrotech.*, 2008, **33**(1), 20–24.
7 Q. L. Jiang, H. Wang, Y. M. Luo, W. Wang, H. X. Wang, J. Gao and K. Zhao, *Initiators Pyrotech.*, 2014, **3**, 42–45.
8 F. Chen, Y. C. Liu, Y. Wang and Q. H. Zhang, *Energetic Mater.*, 2020, **28**, 1109–1119.
9 D. Chavez, L. Hill, M. Hiskey and S. Kinkead, *J. Energ. Mater.*, 2000, **18**, 219–236.
10 V. Pepekin, B. Korsunskii and Y. N. Matyushin, *Combust. Explos. Shock Waves*, 2008, **44**, 110–114.
11 Y. Li, J. M. Yuan, W. Zhao, Y. Qu, X. W. Xing, J. W. Meng and Y. C. Liu, *Russ. J. Gen. Chem.*, 2021, **91**, 445–455.
12 G. Luo, H. Huang, S. Zhang, P. S. Wang, Z. Z. Cai and Y. Zhang, *Energetic Mater.*, 2012, **20**, 437–440.
13 L. Tang, H. Li, Y. Tan, T. Liu and Z. Yang, *CrystEngComm*, 2020, **22**, 2173–2182.
14 L. Chen, Y. J. Shu, R. J. Xu, T. Xu and X. F. Wang, *Energetic Mater.*, 2013, **21**, 108–115.
15 B. B. Li, Y. M. Luo, W. Lei, M. M. Zhang and W. Wang, *Energetic Mater.*, 2021, **29**, 308–314.
16 J. Gao, H. Wang, Y. M. Luo, H. X. Wang and W. Wang, *Chin. J. Explos. Propellants*, 2020, **43**, 213–218+224.

Open Access Article. Published on 20 November 2024. Downloaded on 10/21/2025 6:07:38 AM.
This article is licensed under a Creative Commons Attribution-NonCommercial 3.0 Unported Licence.

17 K. Yang, F. Bi, J. Zhang, Q. Xue, J. Zhang, K. Wang and B. Wang, *Arab. J. Chem.*, 2022, **15**, 103947.
18 Q. Xue, F. Bi, L. Zhai, T. Guo, J. Zhang, S. Zhang, B. Wang and J. Zhang, *ChemPlusChem*, 2019, **84**, 913–918.
19 G. R. Desiraju, *Acc. Chem. Res.*, 1996, **29**, 441–449.
20 D. Trache, K. Khimeche, R. Benelmir and A. Dahmani, *Thermochim. Acta*, 2013, **565**, 8–16.
21 N. E. Beach and V. K. Canfield, 1971.
22 J.-F. Pei, F.-Q. Zhao, H.-L. Lu, X.-D. Song, R. Zhou, Z.-F. Yuan, J. Zhang and J.-B. Chen, *J. Therm. Anal. Calorim.*, 2016, **124**, 1301–1307.
23 Q. L. Yan, X. J. Li, L. Q. Liao, X. H. Zhang and Z. R. Liu, *Energetic Mater.*, 2008, 309–314.
24 Z. R. Liu, *Thermal Analyses of Energetic materials*[M], Beijing, National Defense Industry, 2009, pp. 388–394.
25 X. N. Ren, S. Y. Heng, Y. H. Shao, Z. R. Liu, G. Zhang, X. H. Wang and F. Han, *Energetic Mater.*, 2009, **17**, 455–458.
26 S. J. Chen, *Phase Diagram Analysis and Application*, 2007.
27 C. B. Storm, J. R. Stine and J. F. Kramer, in *Chemistry and Physics of Energetic Materials*, ed. S. N. Bulusu, Springer Netherlands, Dordrecht, 1990, pp. 605–639, DOI: 10.1007/978-94-009-2035-4_27.
28 M. Sućeska, *EXPLO5*, Brodarski Institute, Zagreb, Croatia, 2013, p. 6.
29 K. Zhao, H. Wang, W. Wang, F. Yang, R. P. Liu and Y. J. Zhu, *Chin. J. Explos. Propellants*, 2016, **39**, 68–72.
30 H. X. Wang, F. F. Jiang, H. Wang, Y. M. Luo and J. Gao, *Energetic Mater.*, 2012, **20**, 423–426.
31 H. X. Wang, X. F. Wang, Y. M. Luo and F. F. Jiang, *Energetic Mater.*, 2009, **17**, 183–186.
32 M. Anniyappan, K. Vijay Varma, R. S. Amit and J. K. Nair, *J. Energ. Mater.*, 2020, **38**, 111–125.
33 X. Yang, J. Zhou, X. Xing, Y. Huang, Z. Yan, Q. Xue, X. Wang and B. Wang, *RSC Adv.*, 2020, **10**(44), 26425–26432.
34 Q. L. Yan, Z. W. Song, T. An, X. H. Zhang and F. Q. Zhao, *Chin. J. Explos. Propellants*, 2016, **39**, 1–12.
35 B. H. Zhen, G. Luo, Y. J. Shu and P. S. Wang, *Chem. Ind. Eng. Prog.*, 2013, **32**, 1341–1346.
36 M. A. Parry and H. H. Billon, The viscosity of (molten) rdx/tnt suspensions, *Proceedings of the 18th International Annual Conference of ICT*, 1987, pp. 1–3.
37 W. F. Larsen, A. A. R. DEVELOPMENT and E. C. P. A. N. P. A. DIRECTORATE, *The Use of Low Viscosity 70/30 Octol in Dragon Warheads M224, AD-A053473*, 1977.
38 R. L. Hatch, Method for processing explosives containing 2, 4, 6, 8, 10, 12-hexanitro-2, 4, 6, 8, 10, 12-hexaazatetracyclo [5.5. 0.05, 903, 11]-dodecan (CL-20) with naphthenic and paraffinic oils, *US Pat.*, 6736913, 2004.
39 Y. X. Ou, Z. Meng and J. Q. Liu, *Chem. Ind. Eng. Prog.*, 2007, 1690–1694.
40 H. X. Wang, X. F. Wang and Y. M. Luo, *Explos. Mater.*, 2021, **50**, 1–9.

 © 2024 The Author(s). Published by the Royal Society of Chemistry